



CONTAINER INFLUENCE ON SHRINKAGE UNDER HOT ISOSTATIC PRESSING—I. SHRINKAGE ANISOTROPY OF A CYLINDRICAL SPECIMEN

E. OLEVSKY

Institute for Mechanics and Materials, University of California,
San Diego, 9500 Gilman Drive, La Jolla, CA 92093-0404, U.S.A.

A. MAXIMENKO, S. VAN DYCK, L. FROYEN, L. DELAEY
Katholieke Universiteit Leuven, Metallurgy and Materials Engineering Department,
de Croylaan 2, Leuven (Heverlee), B-3001, Belgium

and

L. BUEKENHOUT

IMT-Europe, 7 Industriepark-Noord, Sint-Niklaas, B-9100, Belgium

(Received 4 December 1996; in revised form 18 June 1997)

Abstract—A mathematical model of isostatic pressing in a cylindrical container is elaborated. The influence of the container geometry, the container and the powder constitutive properties on shrinkage anisotropy (change of the powder specimen's aspect ratio) is analyzed. The idea of using containers with different thicknesses of the lateral and end face walls for controlling the shrinkage anisotropy is suggested. Model experiments on HIPing of copper powder in a copper container are carried out. The design principle of proportionality of the ratio of container wall thicknesses and the ratio of container internal dimensions is analytically derived and experimentally tested. © 1998 Elsevier Science Ltd. All rights reserved.

1. INTRODUCTION

The production of near-net shape components by hot isostatic pressing is one of the actual problems of modern powder technologies. At first glance, one could expect, that the shrinkage of a porous body under conditions of the uniform hydrostatic compression is self-similar, changing only the volume without changing the shape. This assumption, however, turns out to be justified only in the ideal case of homogenous article properties and uniformity of the external load. In practice, for most cases, these conditions are not met, as a result of which the shrinkage becomes variable in different parts of the porous object's volume. Therefore, it is important to identify the crucial factors, having an influence on shrinkage inhomogeneity. Control of these influences can provide the production of near-net shape components.

For hot isostatic pressing, three groups of factors, having an impact on shape formation and receipt of the final configuration of an article, can be distinguished:

- heat influence (in particular, temperature field nonuniformity);
- inhomogeneity of macrostructure parameters (for example, porosity field);
- container influence.

During HIPing a nonuniformity of the temperature field can cause the so-called "densification wave effect", which has been analysed in a number of works (Li *et al.*, 1987, 1991); Li and Easterling, 1992; Olevsky *et al.*, 1994). Owing to the nonuniform initial warming-up of the porous specimen, the hotter outer layers are densified faster, forming a dense skin, which subsequently can impede the shrinkage of the internal part of the porous specimen. The ratio between the velocities of the propagation of temperature and density fronts has been determined by Li *et al.* (1987) as a criterion of this phenomenon existence.

The dependence of the densification wave effect on the nonlinearity of the rheological properties of a matrix phase material (porous body skeleton) was analysed by Olevsky *et al.* (1994). It has been shown that the densification wave appears under considerably high degrees of this nonlinearity only.

Formally, the heterogeneity of the temperature field can be used for production of the requisite final shape of an article by means of application of an evident technical idea of the nonuniform heating of different parts of porous specimen. However, apart from shortcomings connected with the above-mentioned "densification wave effect", considerable difficulties of the technological realization of this idea should be noted.

The use of porous specimens with nonuniformly spatially distributed porosity considered by Maximenko *et al.* (1994) is an example of the application of the second group of factors (heterogeneity of macrostructure parameters) for controlling the final shape of an article. Different parts of the porous specimen, having a different porosity, undergo a different shrinkage during HIPing. In such a manner, for example, a "dumb-bell" shape can be obtained from a cylindrical porous specimen. The necessity of the preliminary preparation of a nonuniformly dense porous specimen, which is a separated technical problem, is a disadvantage of this method.

The container influence is the most essential factor for the formation of the final shape of an article (Wadley *et al.*, 1991). The shrinkage anisotropy, being accompanied by the appearance of the deviatoric stress components in the porous volume, is an important technological consequence of a container use. In some works (Li and Easterling, 1992; McMeeking 1992) this problem is studied for pressing of a powder cylinder in a long tube without considering the influence of the container bottoms. In the works of Besson and Abouaf (1990), and Xu and McMeeking (1992) the deformation of the container is analysed on the basis of the shell theory. It is evident, however, that for hot deformation processes, not only powder viscous-plastic properties' nonlinearity should be taken into consideration, but the nonlinearity of the container viscous-plastic properties as well.

The finite-element method (FEM) provides the most full analysis of the deformation picture of the powder-container system (Besson and Abouaf, 1992; Aboudance *et al.*, 1994; Govindarayan and Aravas, 1994; Jinka *et al.*, 1994; Zahrah *et al.*, 1994).

In HIPing practice, the container are often applied, whose wall thickness is significantly smaller than characteristic dimensions of an article. Therefore, if one single discretization network is used, it is necessary to make it throughout the article as fine as in the volume of container. A considerable amount of the HIPing numerical investigations deals with this approach to the modeling. This is not a good use of computer capacity but otherwise a considerable dimension difference of elements requires special algorithms in order to avoid solution of an ill-conditioned set of equations (Cook, 1974). In addition, the problem is also dramatized by the strong nonlinearity of the material constitutive equations. These troubles are not specific features of the HIPing computer simulation only, but they have crucial importance for the correct shape change prediction in processing at hand. Thereby, the elaboration of simple and highly efficient numerical approaches remains a current challenge for specialists in modeling.

In the present work a modification of the variational principle, being the basis of the FEM for the determination of a field of unknown kinematic parameters (velocities, displacements), is suggested. The modified finite-element algorithm is realized by a simple example of the solution of the problem of HIPing in a cylindrical container. Along with this, the technological idea of using the container with different thicknesses of the lateral and end face walls for controlling the shrinkage anisotropy, is suggested and analysed. The calculation results obtained are compared with the experimental data for HIPing the copper powder in cylindrical copper and steel containers.

2. THE PHENOMENOLOGICAL MODEL OF CONSOLIDATION OF POROUS BODIES

In all the speculations mentioned below, a porous medium is described as a two-phase continuum of a matrix type. Non-linear, incompressible and isotropic properties of the matrix phase are assumed. The second compressible phase comprises voids and determines

the irreversible volume change of the entire porous medium. The deformed solid is regarded as a whole, endowing it with the ability to change not only its shape but also its volume. The macroscopic parameters in rheological relationships, such as stress tensor σ_{ij} , strain rate tensor $\dot{\mathbf{e}}_{ij}$, density ρ , velocity components v_i and other are spatial averages over a representative volume which is much larger than the typical dimension of pores but smaller than the one of the macroscopic porous body considered. The porosity θ is a very important parameter, which can be determined as the ratio of the pores' volume and the total volume of the representative element.

The derivation of the constitutive law for a porous medium can be performed through averaging stresses and strains over a properly chosen unit cell of material. In the case of nonlinear-viscous or rigid-plastic behaviour of the skeleton of porous body, a method of the creep potentials has enjoyed the widest application. The creep or dissipation potential is an extension of the well-known Rayleigh dissipation potential to the nonlinear behaviour of material. Like Rayleigh potential it has some useful mathematical properties. For an isotropic media, the creep potential Φ is a positive and homogeneous function with respect to the invariants of the strain rate tensor. This enables the determination of the average stresses in the medium as follows (Kachanov, 1971):

$$\sigma_{ij} = \frac{\partial \Phi}{\partial \dot{\mathbf{e}}_{ij}} \quad (1)$$

The dissipation potential is related to the energy dissipation rate density in material. If Φ is assumed to be independent of the third invariant of the strain rate tensor, the relationship between the creep potential and the average dissipation rate D has the form (Mosolov and Myasnikov, 1981):

$$\Phi = \int_0^1 D(\kappa e, \kappa \gamma) \frac{d\kappa}{\kappa} \quad (2)$$

where e, γ are the first invariant of the strain rate tensor and the second invariant of the deviator of this tensor, respectively.

The development of constitutive eqn (1) is possible if the average energy dissipation density is known as a function of a porosity, physical parameters of the skeleton of porous body and the average strain rates. The specific form of D for the different topological micromechanical model of the porous body can be obtained only from the comprehensive numerical experiments. For a porous medium, detailed computer calculations proved that an approximation for D is possible in the following form (Sofronis and McMeeking, 1992; Kuhn *et al.*, 1993):

$$D = \sigma_0 \dot{\epsilon}_0 \sqrt{1-\theta} \left[\frac{\sqrt{\psi e^2 + \varphi \gamma^2}}{\dot{\epsilon}_0} \right]^{\alpha+1} \quad (3)$$

The solid constituent (porous body skeleton) is assumed to obey the power law creep under uniaxial loading

$$\sigma = \sigma_0 \left(\frac{\dot{\epsilon}}{\dot{\epsilon}_0} \right)^\alpha \quad (4)$$

where $\sigma, \dot{\epsilon}$ are the stress and the axial strain rate in this case. Generally, relation (4) is controlled by physical mechanism of viscous flow and can be determined by hot isostatic pressing diagrams (Arzt *et al.*, 1983). In general, parameters ψ, φ are functions of porosity and power law exponent α . In the case when $\theta < 2/3$ it is noted (Olevsky *et al.*, 1996) that:

$$\begin{aligned}\varphi &= (1 - \theta)^2 \\ \psi &= 2\varphi(1 - \theta)/3\theta\end{aligned}\quad (5)$$

These expressions for φ and ψ are derived by the extrapolation of the results obtained for the rheologies close to the linear-viscous one.

If eqn (3) is valid, the creep potential has the following form

$$\Phi = \frac{1}{\alpha + 1} D \quad (6)$$

If the matrix material is a strain-hardening one, we stipulate that

$$\sigma_0 = \sigma_1 + \sigma_2 \omega^\beta \quad (7)$$

where σ_1 is an initial yield limit, σ_2 is a coefficient of hardening and β is a degree of hardening. Accumulated deformation ω is a generalization of the Odquist's parameter (Kachanov, 1971) to plasticity of porous bodies. In both cases the derivative of ω with respect to time can be given in the following form:

$$\frac{d\omega}{dt} = \frac{D}{(1 - \theta)\sigma_0} \quad (8)$$

where the dissipation rate D is taken from eqn (3) for $\alpha = 0$. From the physical point of view the validity of eqn (8) results from the feasibility of continuous transformation of porous material into incompressible one with $\theta \rightarrow 0$. For the incompressible plastic material, $\theta = 0$ and $d\theta/dt = 0$. If porosity approaches zero, the first right-hand term in the brackets of eqn (3) tends to zero because $e \rightarrow 0$ and function φ is always specified in a way to provide $\varphi \rightarrow 1$ for $\theta \rightarrow 0$.

The right-hand side of eqn (8) can be considered as a definition of the average strain rate intensity W in the skeleton of a porous body:

$$W = \frac{D}{(1 - \theta)\sigma_0} \quad (9)$$

3. THE EXTREMUM PRINCIPLE FOR CALCULATION OF HIPING IN CONTAINER

The determination of the fields of the unknown kinematic parameters of deformation (in our case they are velocities of the powder and the container, being deformed) is the main component of the wide range of finite-element algorithms, describing deformation processes in continuum medium. For this purpose, the extremum principle can be used, implying the requirement of the extremity of the functional

$$I = \int_{\Omega} \Phi \, d\Omega - \int_{\Omega} \mathbf{F} \cdot \mathbf{v} \, d\Omega - \int_S \mathbf{T} \cdot \mathbf{v} \, dS \quad (10)$$

where Ω is the volume deformed, S is its surface area, \mathbf{F} and \mathbf{T} are body forces and surface traction, respectively, \mathbf{v} is a velocity vector. Based on the most general assumption of the form of Φ , it was obtained by Mosolov and Myasnikov (1981) that the real field of flow velocities imparts minimum value to the functional I :

$$I_{\text{real flow velocities}} \rightarrow \min \quad (11)$$

The most common and widespread HIPing technology is a compaction of powder under the uniform pressure. In this case, the vector of surface traction has only one

component, which is normal to the surface and equal to the external pressure P . After simple arrangements, the surface integral in eqn (10) can be transformed into the volume integral and the extremum principle assumes the following form:

$$I = \int_{\Omega} (\Phi - Pe) d\Omega \quad (12)$$

It should be noted that the dissipation rates and the creep potentials have different forms in the powder and in the container volume. The total volume Ω embraces both constituents of the porous specimen.

4. THE CALCULATION OF THE SHRINKAGE ANISOTROPY UNDER HOT ISOSTATIC PRESSING IN A CYLINDRICAL CONTAINER

Consider the application of the above-mentioned approach for the description of the HIPing of the cylindrical article for the simplest case of a subdivision of the object to be investigated into finite elements. One element corresponds to a powder and two elements correspond to the container, the first one corresponds to the lateral part, and the second one to the bottom (Fig. 1). The above-mentioned scheme excludes the influence of container corners on shrinkage anisotropy. A single influencing geometrical factor is the wall thickness.

Further, the condition of full bonding of the powder and the container is used. As indicated below, in this case the variational functional can be expressed in terms of the two independent variables, which are radial e_r and axial e_z porous specimen strain rates.

4.1. The derivation of the kinetic equations for the volume shrinkage and the porous specimen size evolution

Consider the problem in axisymmetrical formulation. Strain rates of the powder elements have the form:

$$e_{\varphi} = e_r = \frac{\dot{R}}{R}; \quad e_z = \frac{\dot{h}}{h} \quad (13)$$

where \dot{R} and \dot{h} are the rates of change of powder porous specimen radius and height, respectively. From the full bonding condition, the container strain rates are

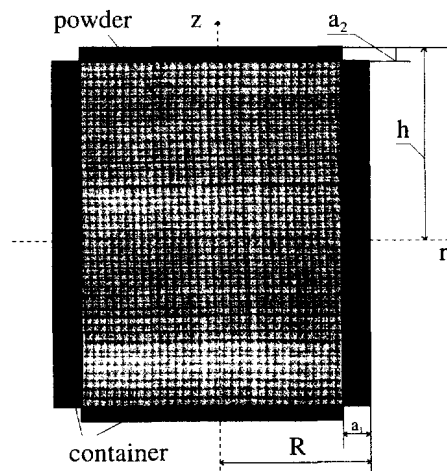


Fig. 1. HIPing of a cylindrical porous specimen in container. The scheme excludes the influence of container corners on the shrinkage anisotropy.

$$e_{rc2} = e_r; \quad e_{zc1} = e_z \quad (14)$$

where indices $c1$ and $c2$ correspond to the lateral and the bottom elements of the container, respectively. The remaining strain rate components have the form

$$e_{rc1} = \dot{a}_1/a_1; \quad e_{zc2} = \dot{a}_2/a_2 \quad (15)$$

where \dot{a}_1 and \dot{a}_2 are the rates of change of the container lateral and bottom thickness, respectively.

From the condition of the volume conservation (see Appendix 1):

$$e_{rc1} = -\frac{Re_r + (R + \frac{1}{2}a_1)e_z}{R + a_1}; \quad e_{zc2} = -2e_r \quad (16)$$

The rate of change of the powder volume is

$$e = e_r + e_\phi + e_z \quad (17)$$

The rate of change of the powder body shape is

$$\gamma = \sqrt{\frac{2}{3}} \sqrt{(e_z - e_r)^2 + (e_z - e_\phi)^2 + (e_\phi - e_r)^2} \quad (18)$$

The expressions, analogous to eqn (29), for the rates of the container elements' shape change γ_{c1} and γ_{c2} can be obtained using the components e_r , e_z and the incompressibility condition for the component e_ϕ .

In accordance with eqn (12), the functional I can be rewritten in the following form:

$$I = I_p + I_{c1} + I_{c2} \quad (19)$$

where I_p corresponds to dissipation in powder, I_{c1} and I_{c2} correspond to dissipation in the lateral and bottom element, respectively. The term I_p has the form eqn (3) with parameters σ_{0p} , α_p and volume of the powder is

$$V_p = 2\pi R^2 h \quad (20)$$

The equation for I_p is conveniently reduced after introducing the following notations and the similar notations n_c , A_c for the parameters of the container.

$$\begin{aligned} n_p &= \alpha_p + 1 \\ A_p &= \sigma_0/n_p \dot{e}_0^2 \end{aligned} \quad (21)$$

In this case, $\Phi = A_p W^{n_p}$, and following eqn (12), I_p can be rewritten as:

$$I_p = \int_{\Omega_p} [A_p W^{n_p} - Pe] d\Omega_p \quad (22)$$

The constituents of the functional eqn (12) associated with the container have the following form:

$$\begin{aligned}
 I_{c1} &= \int_{\Omega_{c1}} A_{c1} \gamma_{c1}^{n_c} d\Omega_{c1} \\
 I_{c2} &= \int_{\Omega_{c2}} A_{c2} \gamma_{c2}^{n_c} d\Omega_{c2}
 \end{aligned} \tag{23}$$

The volume of the lateral part of the container is:

$$V_{c1} = 2\pi((R+a_1)^2 - R^2)h \tag{24}$$

and the volume of the bottom part is:

$$V_{c2} = 2\pi R^2 a_2 \tag{25}$$

Taking into consideration eqns (17), (18), (20), (24), (25), the eqns (22), (23) assume the form:

$$\begin{aligned}
 I_p &= 2\pi R^2 h \left\{ A_p \left[\frac{1}{\sqrt{1-\theta}} \sqrt{\psi(2e_r + e_z)^2 + \frac{4}{3}\varphi(e_z - e_r)^2} \right]^{n_p} - P(2e_r + e_z) \right\} \\
 I_{c1} &= 2\pi a_1 (2R + a_1) h A_c \left\{ \frac{2}{3(R+a_1)^2} \left[\left(R e_r + \left(2R + \frac{3}{2} a_1 \right) e_z \right)^2 + R^2 (2e_r + e_z)^2 \right. \right. \\
 &\quad \left. \left. + \left(R e_r - \left(R + 3 \frac{a_1}{2} e_z \right)^2 \right) \right] \right\}^{n_c/2} \\
 I_{c2} &= 2\pi R^2 a_2 A_c \{ 2\sqrt{3e_r^2} \}^{n_c}
 \end{aligned} \tag{26}$$

In this case, the Euler equations for the extremum principle eqn (12) are given by:

$$\begin{aligned}
 \frac{\partial I}{\partial e_r} &= 0 \\
 \frac{\partial I}{\partial e_z} &= 0
 \end{aligned} \tag{27}$$

Substituting eqns (19) and (26) into eqn (27), we obtain (see Appendix 2):

$$\begin{aligned}
 &\left[4\lambda_p \left(\psi + \frac{\varphi}{3} \right) 2\lambda_{c1} R^2 + \lambda_{c2} \right] e_r + \left[2\lambda_p \left(\psi - \frac{2\varphi}{3} \right) + \lambda_{c1} R^2 \right] e_z - 2V_p P = 0 \\
 &\left[2\lambda_p \left(\psi - \frac{2\varphi}{3} \right) + \lambda_{c1} R^2 \right] e_r + \left[\lambda_p \left(\psi + \frac{4\varphi}{3} \right) + \lambda_{c1} \left(2R^2 + 3a_1 R + \frac{3}{2} a_1^2 \right) \right] e_z - V_p P = 0
 \end{aligned} \tag{28}$$

where

$$\begin{aligned}\dot{\lambda}_p &= \frac{4\pi R^2 h A_p n_p}{(1-\theta)^{n_p/2}} \left[\psi \left(2e_r + e_z \right)^2 + \frac{4\varphi}{3} (e_z - e_r)^2 \right]^{(n_p/2)-1} \\ \lambda_{c1} &= 12\pi a_1 \left(2R + a_1 \right) h A_c n_c \left[\frac{\sqrt{6}}{3(R+a_1)} \right]^{n_c} \left[\left(R e_r + \left(2R + \frac{3}{2} a_1 \right) e_z \right)^2 + R^2 (2e_r + e_z)^2 \right. \\ &\quad \left. + \left(R e_r - \left(R + \frac{3a_1}{2} \right) e_z \right)^2 \right]^{(n_c-2)/2} \\ \lambda_{c2} &= 4\pi R^2 a_2 A_c n_c (2\sqrt{3})^{n_c} (e_r)^{n_c-2}\end{aligned}\quad (29)$$

In general case, eqn (28) is a set of nonlinear equations with unknown e_r , e_z , and λ_p , λ_{c1} , λ_{c2} are the functions of e_r , e_z too. For solving eqn (28), an explicit iteration procedure is used. The obtained values of the strain rates are substituted into the set of the ordinary differential equations in order to determine five functions of time: $R(t)$, $h(t)$, $a_1(t)$, $a_2(t)$, $\theta(t)$.

$$\begin{aligned}\frac{dR}{dt} &= R e_r \\ \frac{dh}{dt} &= h e_z \\ \frac{da_1}{dt} &= -a_1 \frac{R e_r + \left(R + \frac{a_1}{2} \right) e_z}{R + a_1} \\ \frac{da_2}{dt} &= -2e_r a_2 \\ \frac{d\theta}{dt} &= (1-\theta)(2e_r + e_z)\end{aligned}\quad (30)$$

The last equation corresponds to the continuity condition for a powder material.

4.2. Influence of the container geometry on shrinkage anisotropy

An analysis of the evolution of the ratio e_r/e_z in the capacity of one of the criteria of shrinkage anisotropy is of interest here. It follows from eqn (28), that

$$\frac{e_r}{e_z} = 1 + \frac{3\lambda_{c1}(R+a_1)^2 - \lambda_{c2}}{4\lambda_p + \lambda_{c2}} \quad (31)$$

In the case of linear-viscous properties of powder and container ($n_p = n_c = 2$), λ_p , λ_{c1} , λ_{c2} do not depend on the strain rates. In general, these coefficients depend on e_r , e_z .

The equation $e_r/e_z = 1$ can be accepted as a criterion of an isotropic shrinkage. Expressing the right-hand part of eqn (31) in terms of the ratio e_r/e_z and setting this value equal to unit for both parts of eqn (31), one can obtain:

$$\frac{a_1}{a_2} = \left[\frac{\left(1 + \frac{a_1}{R} \right)^2}{9 \left(2 + \frac{a_1}{R} + \frac{1}{2} \left(\frac{a_1}{R} \right)^2 \right)} \right]^{(n_c/2)-1} \frac{(3\sqrt{2})^{n_c}}{9 \left(2 + \frac{a_1}{R} \right) \frac{h}{R}} \quad (32)$$

In the general case, eqn (32) is a criterion of "instantaneous" isotropy.

For the case of linear-viscous properties of the container material ($n_c = 2$), (32) is transformed into the form:

$$\frac{a_1}{a_2} = \frac{2}{\left(2 + \frac{a_1}{R}\right) \frac{h}{R}} \quad (33)$$

For the ideal plastic properties of the container material ($n_c = 1$):

$$\frac{a_1}{a_2} = \frac{\sqrt{\left(1 + \frac{a_1}{R}\right)^2 + 3}}{\left(1 + \frac{a_1}{R}\right) \left(2 + \frac{a_1}{R}\right) \frac{h}{R}} \quad (34)$$

For a small lateral wall thickness ($a_1/R \ll 1$), we obtain a simple relationship for any container rheology ($1 \leq n_c \leq 2$)

$$\frac{a_1}{a_2} \approx \frac{h}{R} \quad (35)$$

which can be, apparently, used as a first approximation for container design.

Thus, for the above mentioned case, in order to avoid shrinkage anisotropy, the ratio between container wall thicknesses should be proportional to the ratio of the dimensions of the internal space of the container in the directions perpendicular to these walls. As follows from eqns (33) and (34), in order to avoid anisotropy, the ratio between bottom and lateral wall thickness has to be increased when the ratio between the lateral wall thickness and container radius increases.

For a wall thickness, which does not satisfy the condition $a_1/R \ll 1$, as a consequence of eqns (32)–(34) we have

$$\frac{\bar{a}_2}{\bar{a}_1} \leq 1 \quad (36)$$

where $\bar{a}_1 = a_1/R$ is the relative thickness of the lateral wall, $\bar{a}_2 = a_2/h$ is the relative thickness of the bottom. The last inequality means that the relative bottom thickness could always be larger than the relative thickness of the lateral wall to avoid anisotropy of shrinkage.

It follows from eqn (36):

$$1 \leq \frac{\left(2 + \frac{a_1}{R}\right)}{2} \leq \left[\frac{9 \left(2 + \frac{a_1}{R} + \frac{1}{2} \left(\frac{a_1}{R}\right)^2\right)}{\left(1 + \frac{a_1}{R}\right)^2} \right]^{(n_c/2)-1} \frac{9 \left(2 + \frac{a_1}{R}\right)}{(3\sqrt{2})^{n_c}} \leq \frac{\left(1 + \frac{a_1}{R}\right) \left(2 + \frac{a_1}{R}\right)}{\sqrt{\left(1 + \frac{a_1}{R}\right)^2 + 3}} \quad (37)$$

that is

$$1 \leq \left(\frac{\bar{a}_2}{\bar{a}_1}\right)_{\text{linear-viscous case}} \leq \left(\frac{\bar{a}_2}{\bar{a}_1}\right)_{\text{nonlinear case}} \leq \left(\frac{\bar{a}_2}{\bar{a}_1}\right)_{\text{ideal plastic case}} \quad (38)$$

The latter means that with increasing of the nonlinearity of the container material properties the deviation of the container geometry from the “equi-thickness” case becomes larger. Inverting this statement, we can conclude that for the highly nonlinearity of the container material properties, the intensity of anisotropy is bigger.

As may be seen from eqns (31) and (32), the rheological properties of the powder do not influence the sign and existence of an isotropy on their own. They have impact only on the intensity of the deviation from an isotropic case.

It is of interest to determine the influence of the nonlinearity of the powder rheological properties on the value of this deviation. In accordance with eqn (31), the intensity of shrinkage anisotropy is inversely proportional to the value of λ_p . Therefore, a relationship between λ_p and the exponent n_p should be determined. From eqn (29) it follows that this relationship depends on a current value of W , e.g. on the current process velocity. It can be shown that for a low speed process, when (see Appendix 3):

$$W < \sqrt{\exp(-2)} 10^{-6} \exp\left(\frac{-Q_{cp}}{R_g T_m} \left(\frac{T_m}{T} - 2\right)\right) \frac{1}{\text{sec}} \quad (39)$$

the higher nonlinearity of the powder properties promotes the lower intensity of anisotropy. For a high-speed process, when

$$W > \sqrt{\exp(-2)} 10^{-6} \exp\left(\frac{-Q_{cp}}{R_g T_m} \left(\frac{T_m}{T} - 2\right)\right) \frac{1}{\text{sec}} \quad (40)$$

the lower intensity of anisotropy corresponds to the more linear powder material properties.

5. SAMPLE CALCULATIONS FOR VOLUME SHRINKAGE AND RESULTS OF THE EXPERIMENTS ON HIPING

Consider a process of hot isostatic pressing of copper powder in a stainless steel container. The input parameters used in accordance with Ashby (1990) are given in the Appendix 4.

The results of the calculations for the different powder porous specimen and container sizes are represented in Fig. 2. The calculation data lend support to the container design idea expressed by eqn (35). The results in Fig. 3 and 4 correspond to the calculations of the hot isostatic pressing of copper powder in a copper container. The data represented in Fig. 3a are obtained for the initial sizes of the container corresponding to those used in the experiments of Wadley *et al.* (1991). Here the wall thickness is accepted to be 2 mm.

For this case, the evolution of the ratio between the diameter and length change is represented in Fig. 3b. This value, which is accepted as a constant in the above-mentioned work of Wadley *et al.*, being initially 2.0, reaches in the end of the process the value of 2.4, which is close to the value 2.5 pointed out by Wadley *et al.* (1991).

As it follows from Fig. 4, the intensity of the shrinkage anisotropy for pressing in a copper container is smaller than in the case of pressing in a steel container. This confirms the idea of lower intensity of the shrinkage anisotropy for the lower nonlinearity of the container material properties.

An idea of using a container with different wall and bottom thickness has been analysed in a number of experiments on hot isostatic pressing of copper in a copper cylindrical container. In order to avoid the container corners' influence, a can with one cornerless end face has been produced (Fig. 5). The corners are absent at the second end face because of the necessity of the placement of the vacuumization system. In doing so, it is assumed that, in view of the long axial size of the container, deformations of the different end faces can be considered to be independent of one another. Thus, after HIPing, change of sizes of the free cornerless end face was analysed.

For the same initial sizes of the container, the same pressure, time and different temperatures, two experiments were carried out (Table 1). The containers were produced in accordance with the design relationship eqn (35). The comparative data on the final sizes

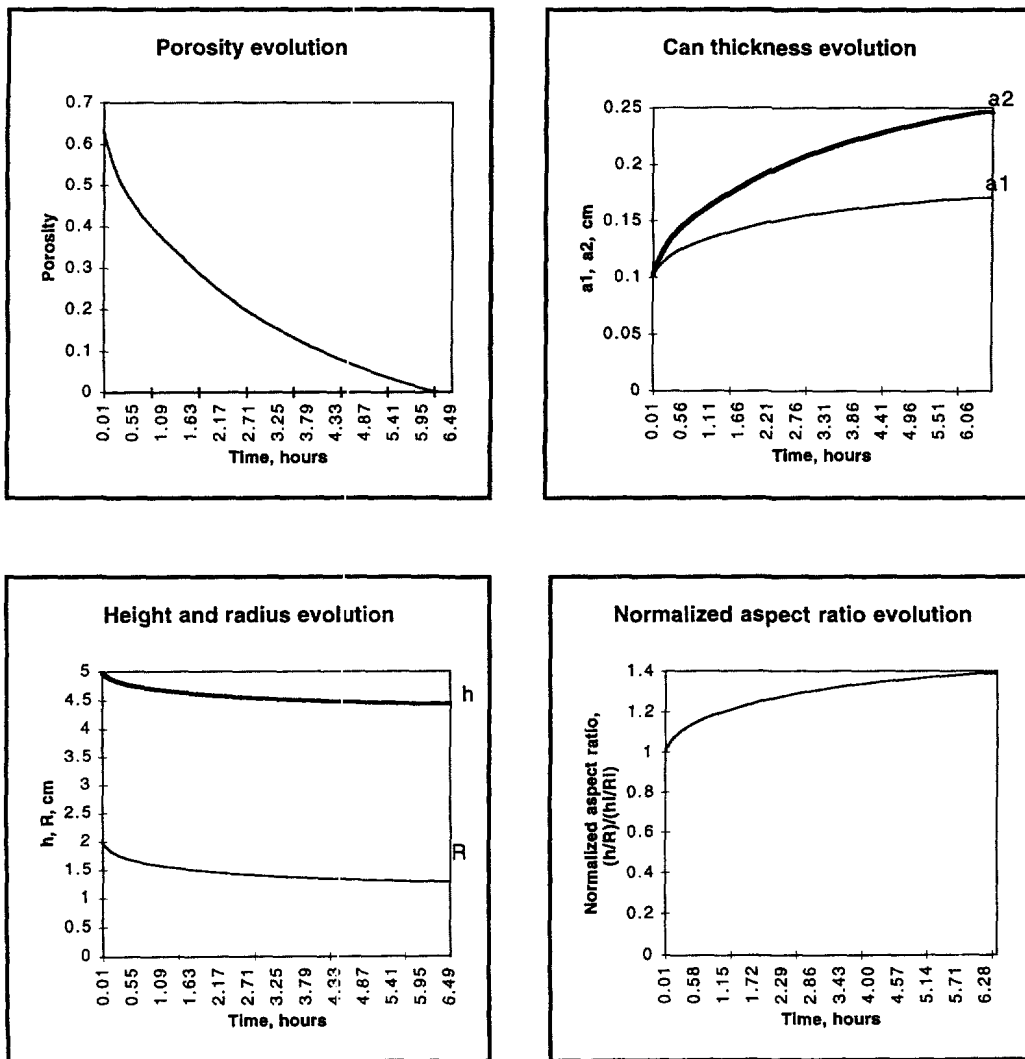


Fig. 2. Shrinkage kinetics and container size evolution. HIPing pressure is 100 MPa, temperature is 750°C; copper powder, stainless steel container: (a) equal bottom and lateral wall thicknesses; (b) proportional bottom and lateral wall relative thicknesses (in accordance with eqn (35)); and (c) inversely proportional bottom and lateral wall relative thicknesses—highest deviation from the isotropic shrinkage.

of the container elements and the final porosity, corresponding to the experiments and the model calculations are represented in Table 2.

By and large, the experiment indicates that, for reaching shrinkage isotropy, the idea of proportionality of the ratio between container wall thickness and the ratio of the dimensions of the internal space of the container in the perpendicular to these walls directions is justified. Some deviations of the final values of the normalized aspect ratio from unit can be explained by the influence of the deformation of the end face with corners on the deformation of the cornerless end face as well as by the approximate character of expression eqn (35). The analysis of container corner's influence on shrinkage anisotropy under isostatic pressing will be a topic of investigations represented in the second part of this paper (Olevsky and Maximenko, 1998).

Acknowledgements—Drs Olevsky and Maximenko acknowledge a Research Fellowship of the Katholieke Universiteit Leuven. The support of Dr Olevsky by the NSF Institute for Mechanics and Materials, University of California, San Diego is gratefully acknowledged.

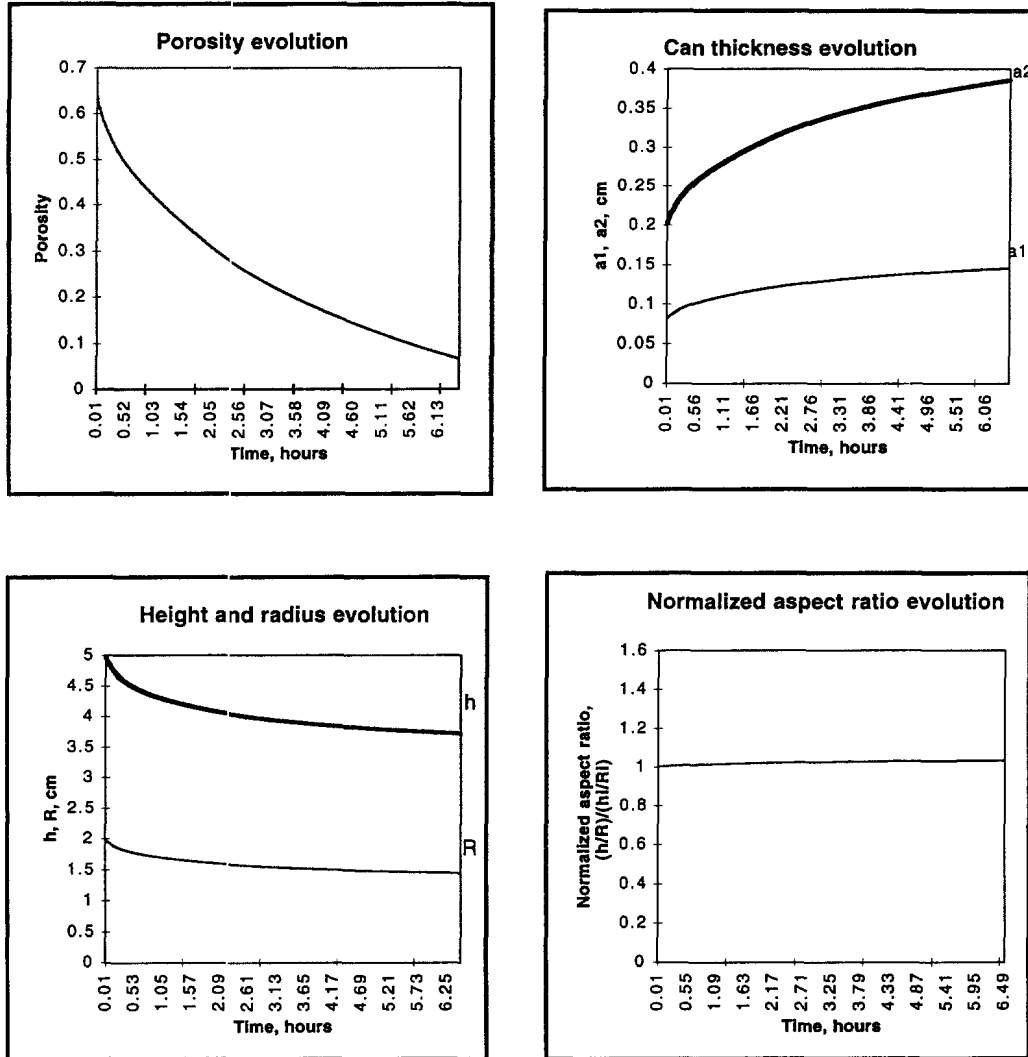


Fig. 2.—Continued.

Table 1. Initial HIPing parameters for the experiments and the calculations

	Initial internal length, mm	Initial internal diameter, mm	Initial wall thickness of the can, mm	Initial bottom thickness of the can, mm	Initial porosity	Temperature, C Pressure, MPa Time, min
(a) Experiment	140	28	2	10	38	750 100 120
(b) Experiment	140	28	2	10	38	900 100 120

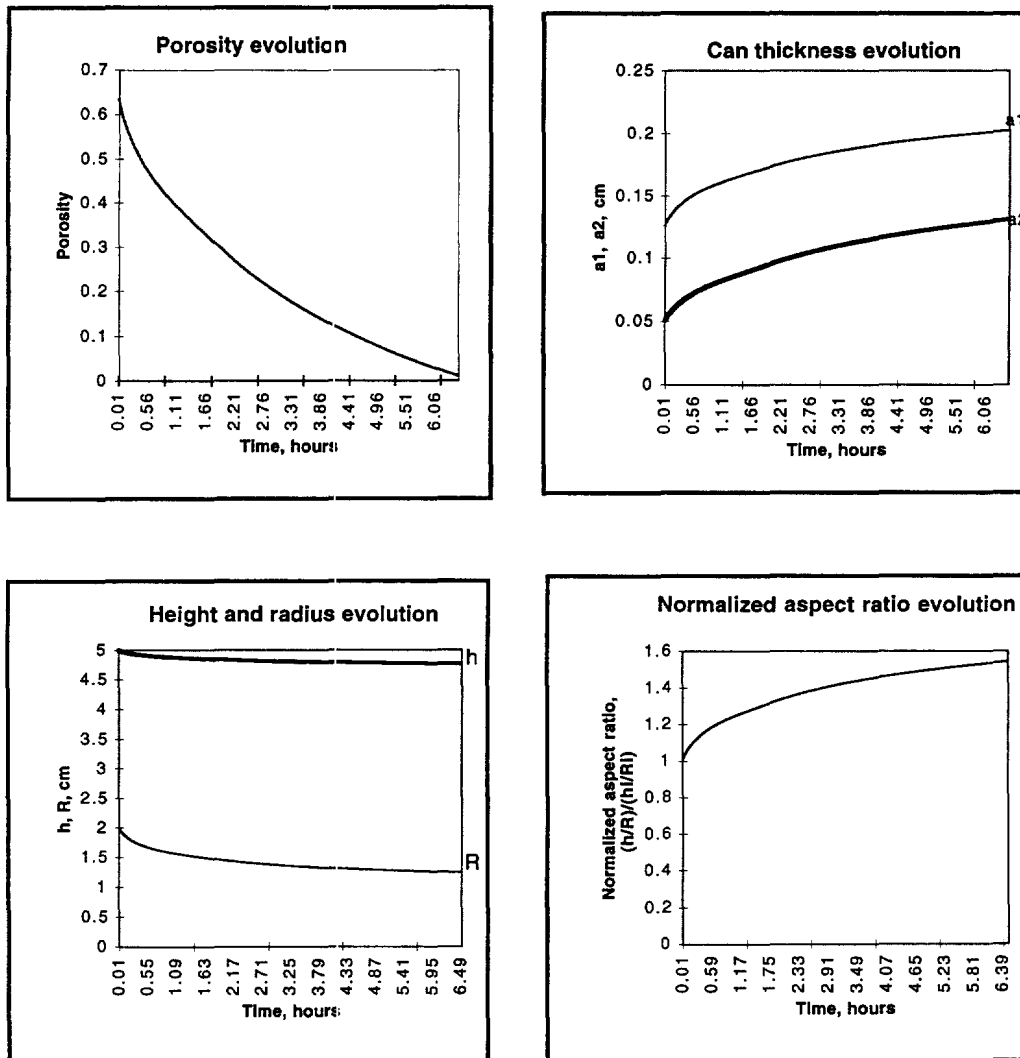


Fig. 2.—Continued.

Table 2. Final porosity and container sizes for the experiments and the calculations

(b) Experiment/model	(a) Experiment/model	
125.21/123.17	134.72/129.44	Final internal length, mm
23.11/23.91	26/25.63	Final internal diameter, mm
2.84/2.60	2.25/2.33	Final wall thickness of the can, mm
10.11/13.39	10.14/11.79	Final bottom thickness of the can, mm
0.00/0.03	0.25/0.20	Final porosity
1.074/1.03	1.036/1.01	Final normalized aspect ratio

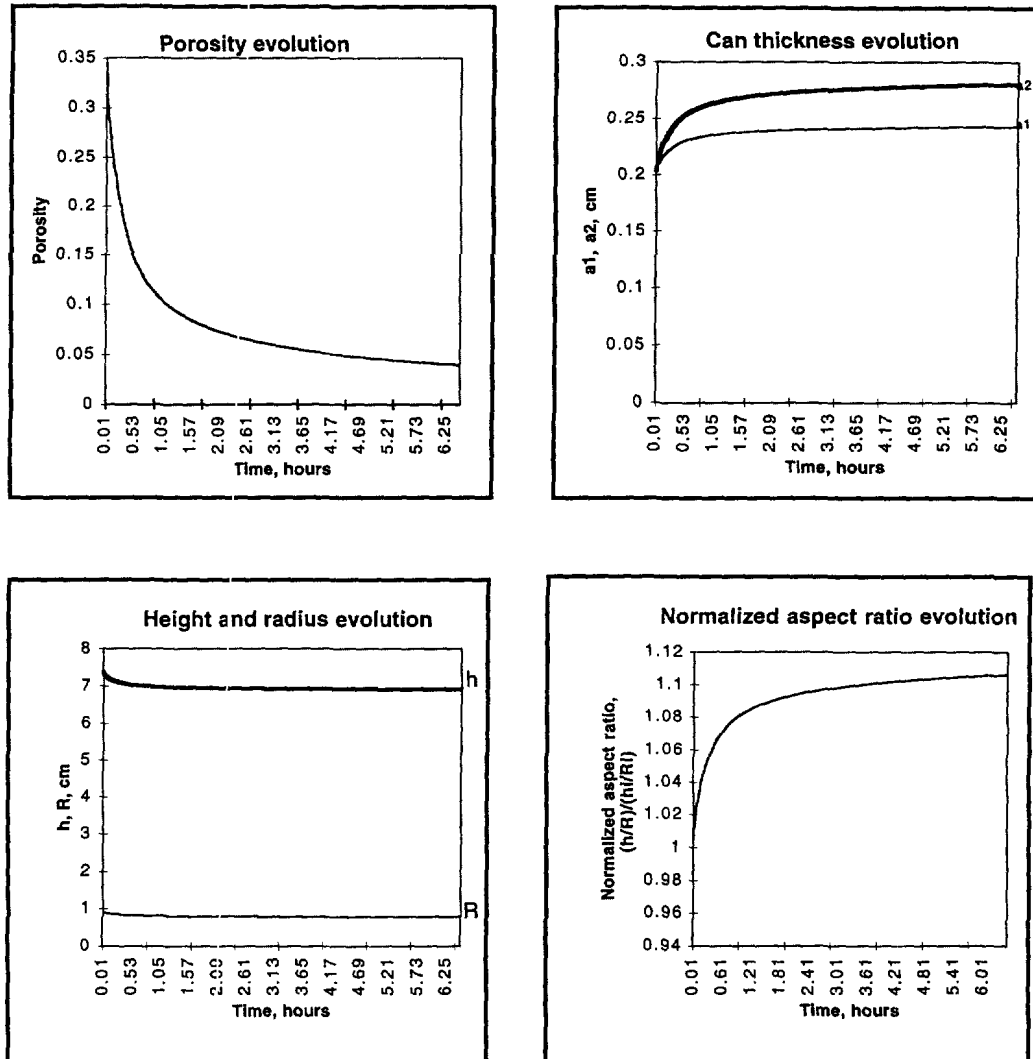


Fig. 3. Calculations for the conditions of the experiment of Wadley *et al* (1991). HIPing pressure is 75 MPa, temperature is 550°C; copper powder, copper container; (a) shrinkage kinetics and container size evolution; and (b) evolution of the ratio between the length and diameter change (a constant value of 2.5 is accepted for this ratio in the paper of Wadley *et al* (1991)).

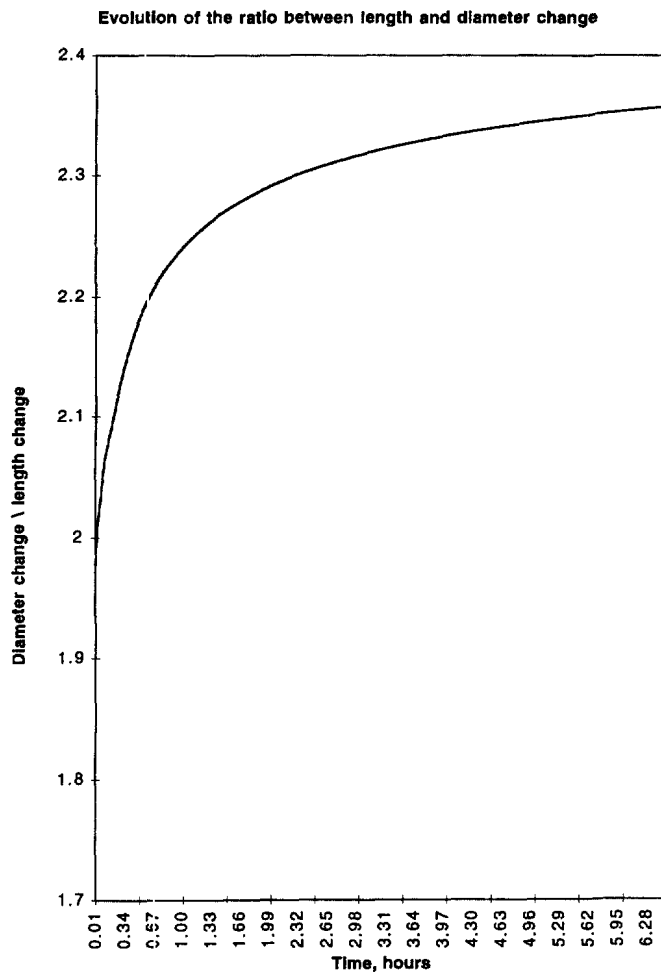


Fig. 3.—Continued.

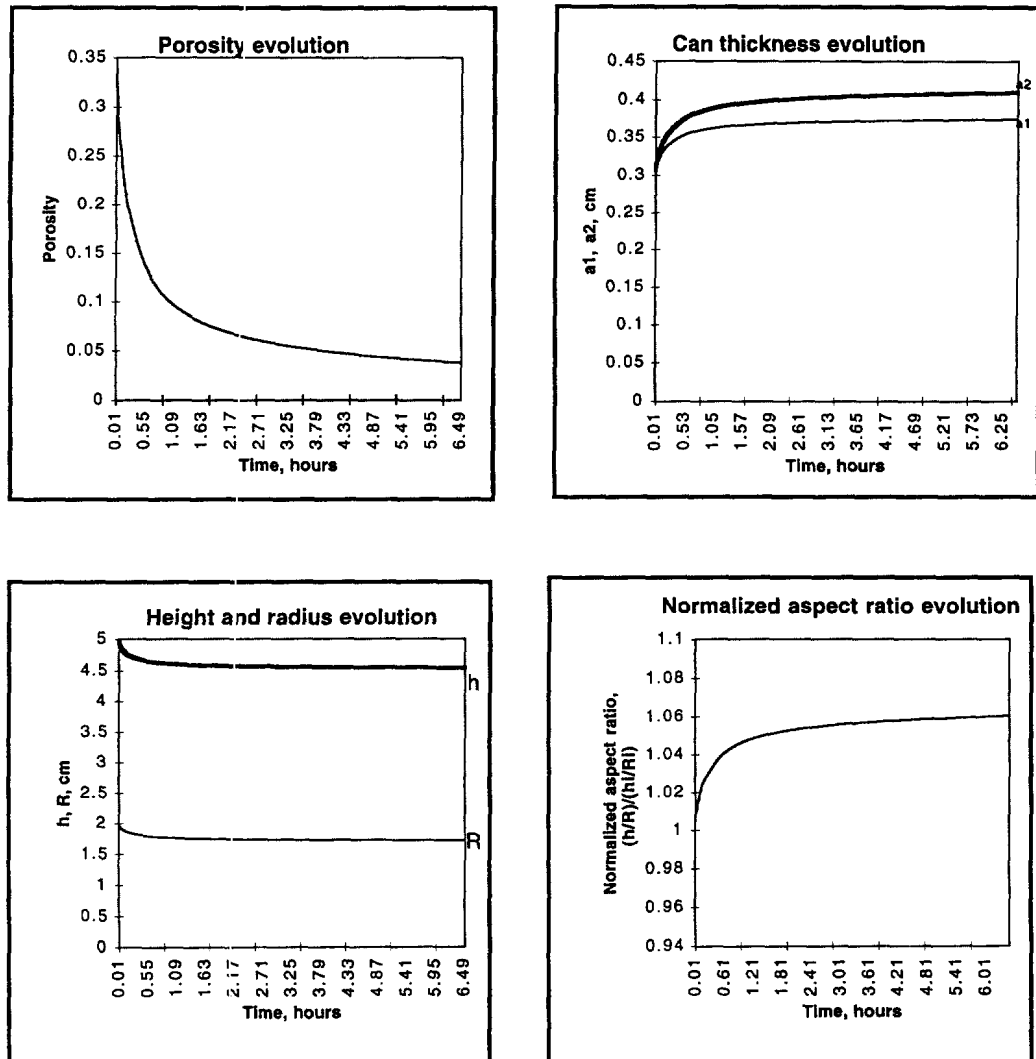


Fig. 4. Shrinkage kinetics and container size evolution. HIPing pressure is 75 MPa, temperature is 550°C; copper powder, copper container; (a) equal bottom and lateral wall thicknesses; (b) proportional bottom and lateral wall relative thicknesses (in accordance with eqn (35)); and (c) inversely proportional bottom and lateral wall relative thicknesses—highest deviation from the isotropic shrinkage.

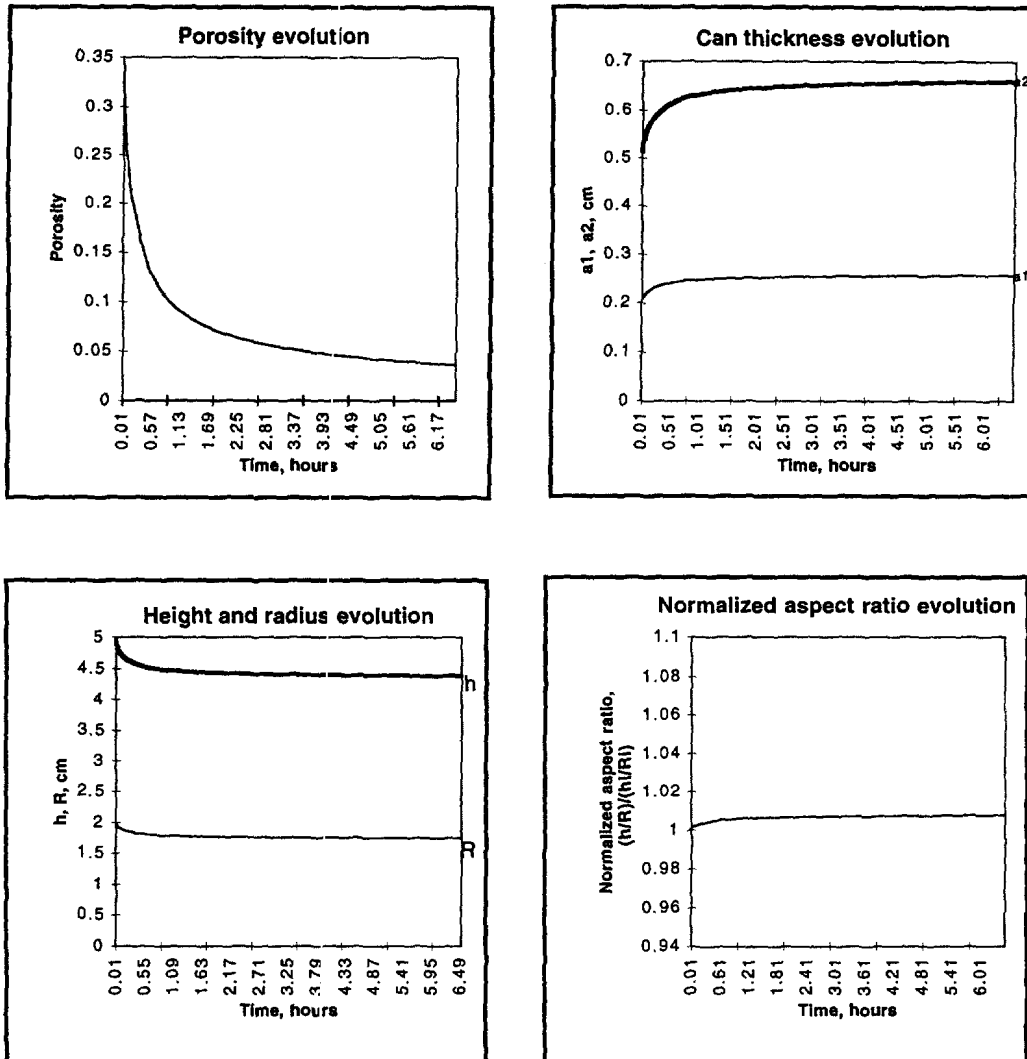


Fig. 4.—Continued.

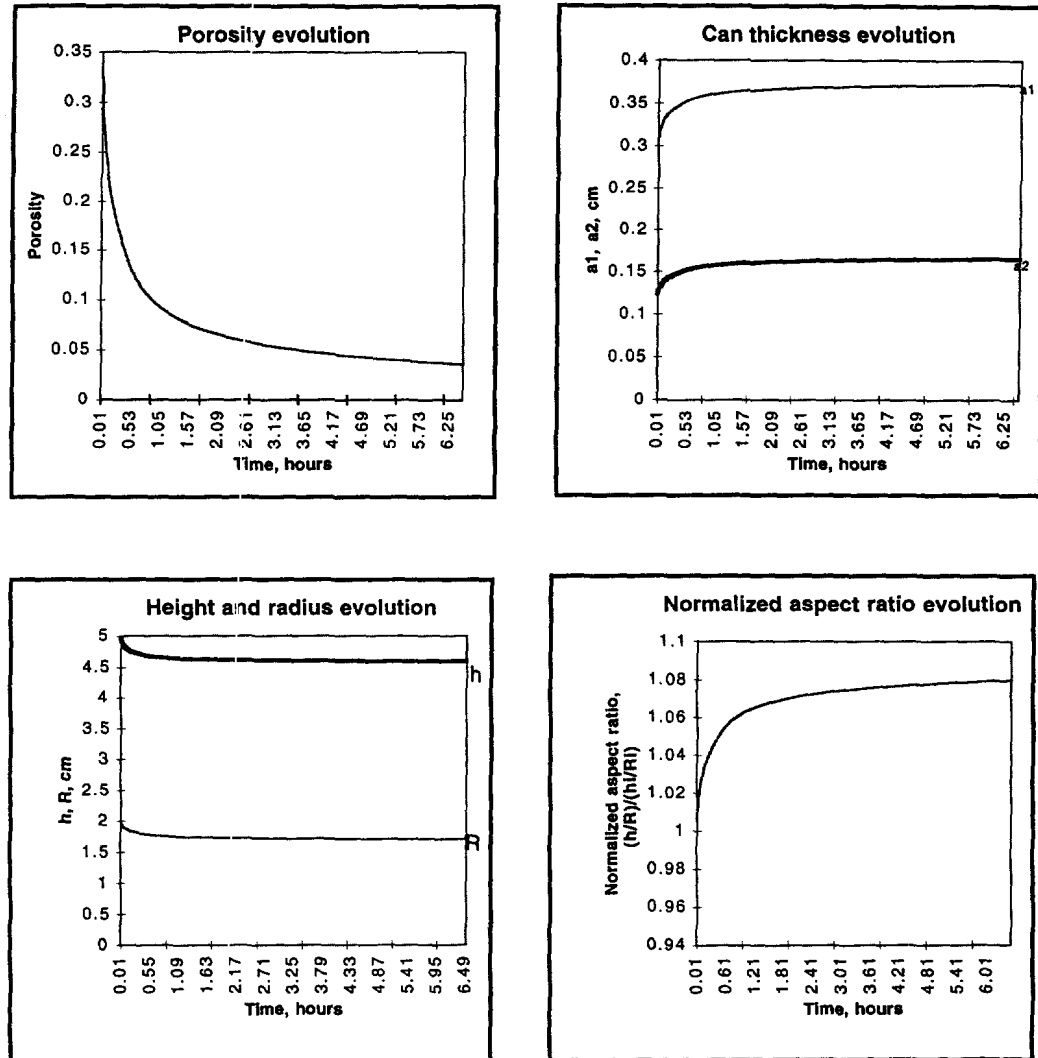


Fig. 4.—Continued.

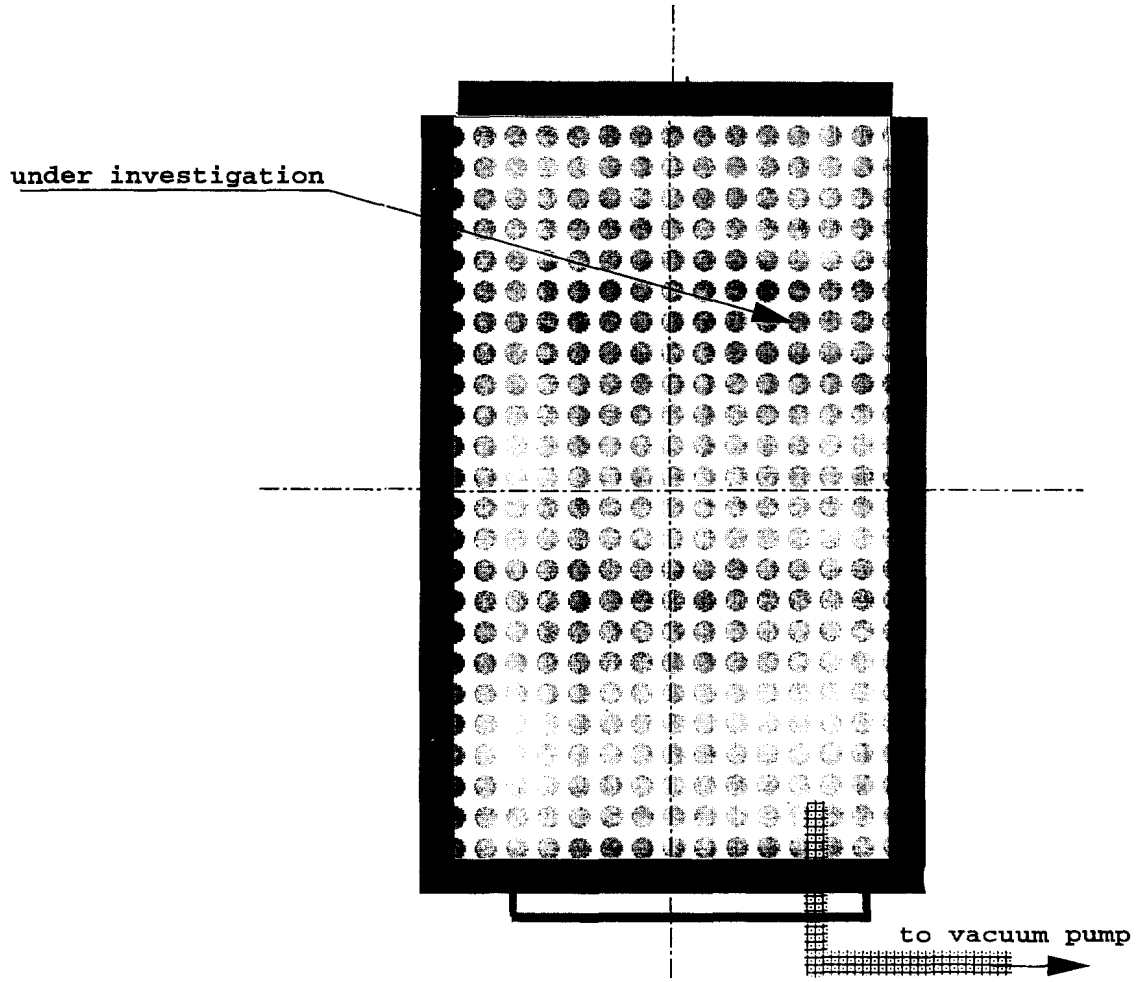


Fig. 5. Design schematic for a cornerless container. Deformations of the different end faces are assumed to be independent of one another.

REFERENCES

- Aboundance, D., Baccino, R. *et al.* (1994) Numerical modelling of near-net shape HIPing of TA6V powder. *Proceedings of the Powder Metallurgy World Congress*, Paris, Les éditions de physique Les Ulis, 797–800.
- Arzt, E., Ashby, M. F. and Easterling, K. E. (1983) Practical applications of hot isostatic pressing diagrams: four case studies. *Metallurgical Transactions* **14A**, 2.
- Ashby, M. F. (1990) HIP 6.0, *Background Reading*, Cambridge University, Engineering Department, U.K.
- Besson, J. and Abouaf, M. (1990) Behavior of cylindrical HIP containers. *International Journal of Solids and Structures* **28**, 6.
- Besson, J. and Abouaf, M. (1992) Rheology of porous alumina and simulation of hot isostatic pressing. *Journal of the American Ceramic Society* **75**, 8.
- Cook, R. D. (1974) *Concepts and Applications of Finite Element Analysis*, Wiley, New York.
- Govindarayan, R. M. and Aravas, N. (1994) Finite element analysis of cold- and hot-isostatic pressing, *Proceedings of the International Conference on Hot Isostatic Pressing*, Antwerp, 1993, (Edited by L. Delaey, H. Tas), pp. 29–36. Elsevier Science B. V., Amsterdam.
- Jinka, A. K. G., Bellet, M. and Fourment, C. (1994) A three-dimensional finite-element simulation of hot powder forging of an automotive part. *Proceedings of the Powder Metallurgy World Congress*, Paris, Les éditions de physique Les Ulis, 793–796.
- Kachanov, L. M. (1971) *Foundations of the Theory of Plasticity*, North-Holland, Amsterdam.
- Kuhn, L., Xu, J. and McMeeking, R. (1993). Constitutive models for the deformation of powder compacts. *Computational & Numerical Techniques in Powder Metallurgy* (Edited by D. Madan, I. Anderson, W. Fraizer, P. Kumar and M. McKimpson), pp. 123–126. The Minerals, Metals & Materials Society.
- Li, W.-B., Ashby, M. F. and Easterling, K. E. (1987) On densification and shape change during hot isostatic pressing. *Acta Metallurgica* **35**, 12.
- Li, W.-B., Easterling, K. E. and Ashby, M. F. (1991) Instantaneous and residual stresses developed in hot isostatic pressing of metals and ceramics. *Metallurgical Transactions* **22A**, 5.
- Li, W.-B. and Easterling, K. E. (1992) Cause and effect of non-uniform densification during hot isostatic pressing. *Powder Metallurgy* **35**, 1.
- Maximenko, A. L., Olevsky, E. A., Pantilor, Y. and Shtern, M. (1994) Compacting of complex-form powder details by isostatic pressing of porous billets with density nonuniformity. *Proceedings of the International Conference on Hot Isostatic Pressing*, Antwerp, 1993 (Edited by L. Delaey and H. Tas), pp. 61–67. Elsevier Science B.V., Amsterdam.
- McMeeking, R. M. (1992). The analysis of shape change during isostatic pressing. *International Journal of Mechanical Science* **34**, 1.
- Mosolov, P. P. and Myasnikov, V. P. (1981) *Mechanics of Rigid-Plastic Media*. Nauka, Moscow.
- Olevsky, E., Shtern, M. and Skorohod, V. (1994) Macroscopic simulation of the consolidation during hot isostatic pressing. *Proceedings of the International Conference on Hot Isostatic Pressing*, Antwerp, 1993 (Edited by L. Delaey and H. Tas), pp. 45–52. Elsevier Science B.V., Amsterdam.
- Olevsky, E., Dudek, H. J. and Kaysser, W. A. (1996) HIPing conditions for processing of metal matrix composites using continuum theory for sintering I. Theoretical analysis. *Acta Metallurgica et Materialia* **44**, N2, 707–713.
- Olevsky, E. and Maximenko, A. (1998) Container influence on shrinkage under hot isostatic pressing—II. Shape distortion of cylindrical specimens. *International Journal of Solids and Structures* **35**, 2035–2314.
- Wadley, H. N. G., Schaefer, R. J. *et al.* (1991) Sensing and modelling of hot isostatic pressing of copper powder. *Acta Metallurgica* **39**, 5.
- Sofronis, P. and McMeeking, R. M. (1992) Creep of power-law material containing spherical voids. *Transactions of the ASME Journal of Applied Mechanics* **59**, 6.
- Xu, J. and McMeeking, R. M. (1992) An analysis of the can effect in an isostatic pressing of copper powder, *International Journal of Mechanical Science* **34**, 2.
- Zahrah, T. F., Charron, F. and Christodoulou, L. (1994) Modeling of consolidation for near-net-shape processing. *Proceedings of the Powder Metallurgy World Congress*, Paris, Les éditions de physique Les Ulis, 783–787.

APPENDIX 1

The volume conservation condition for the container lateral element :

$$\frac{d}{dt}[2\pi h((R+a_1)^2 - R^2)] = 0 \Rightarrow [2(R+a_1)\dot{a}_1 + 2a_1\dot{R}]h + a_1(2R+a_1)\dot{h} = 0 \Rightarrow$$

$$\Rightarrow \frac{\dot{a}_1}{a_1} = -\frac{R\dot{R} + \left(R + \frac{a_1}{2}\right)\frac{\dot{h}}{h}}{R+a_1} \Rightarrow e_{rc1} = -\frac{Re_r + \left(R + \frac{a_1}{2}\right)e_z}{R+a_1}$$

The volume conservation condition for the container bottom element :

$$\frac{d}{dt}[2\pi R^2 a_2] = 0 \Rightarrow \frac{\dot{a}_2}{a_2} = -2\frac{\dot{R}}{R} \Rightarrow e_{rc2} = -2e_r$$

APPENDIX 2

Taking into consideration expression (19), equation (27) can be represented as follows :

$$\frac{\partial I_p}{\partial e_r} + \frac{\partial I_{c1}}{\partial e_r} + \frac{\partial I_{c2}}{\partial e_r} = 0$$

$$\frac{\partial I_p}{\partial e_z} + \frac{\partial I_{c1}}{\partial e_z} + \frac{\partial I_{c2}}{\partial e_z} = 0$$

In virtue of eqn (26), the partial derivatives in the latter relationships are given by :

$$\frac{\partial I_2}{\partial e_r} = 4\lambda_p \left(\psi + \frac{1}{3}\varphi \right) e_r + 2\lambda_p \left(\psi - \frac{2}{3}\varphi \right) e_z - 2V_p P$$

$$\frac{\partial I_{c1}}{\partial e_r} = \lambda_{c1} R^2 (2e_r + e_z)$$

$$\frac{\partial I_{c2}}{\partial e_1} = \lambda_{c2} e_r$$

$$\frac{\partial I_p}{\partial e_z} = 2\lambda_p \left(\psi - \frac{2}{3}\varphi \right) e_r + \lambda_p \left(\psi + \frac{4}{3}\varphi \right) e_z - V_p P$$

$$\frac{\partial I_c}{\partial e_z} = \lambda_{c1} R^2 e_r + \lambda_{c1} \left(2R^2 + 3a_1 R + \frac{3}{2} a_1^2 \right) e_z$$

$$\frac{\partial I_{c3}}{\partial e_z} = 0$$

APPENDIX 3

Following Ashby (1990), the relationship between the equivalent stress σ and the equivalent strain rate W can be determined:

$$W = \left[\frac{\sigma}{\sigma_{ref}} \right]^m \exp \left\{ \frac{-Q_c}{R_g T_m} \left(\frac{T_m}{T} - 2 \right) \right\} 10^{-6} \frac{1}{\text{sec}}$$

where σ_{ref} is the reference stress for power-law creep, MPa; m is the power-law creep exponent; Q_c is the activation energy, KJ/mol; R_g is the gas constant; T_m is the melting point, K; T is temperature, °K. Transform the last equation into the form $\sigma = AW^n$ used in our derivations:

$$\sigma = \sigma_{ref} \exp \left\{ \frac{Q_c}{R_g T_m m} \left(\frac{T_m}{T} - 2 \right) \right\} (10^6 \text{ sec } W)^{1/m}$$

For our designation:

$$A = \sigma_{ref} \left[10^6 \text{ sec} \cdot \exp \left\{ \frac{Q_c}{R_g T_m} \left(\frac{T_m}{T} - 2 \right) \right\} \right]^{1/m}; \quad n = \frac{1}{m} + 1$$

APPENDIX 4

The input parameters for a copper powder:

$$\sigma_{ref} = 35 \text{ MPa};$$

$$T_m = 1356 \text{ K};$$

$$Q_{cp} = \begin{cases} 0.65 \cdot \text{KJ/mol} & \text{if } T < 600 \text{ K} \\ 197 \text{ KJ/mol}, & \text{if } T > 600 \text{ K} \end{cases}$$

$$n_p = 1.21$$

for a stainless steel container

$$\sigma_{ref} = 220 \text{ MPa};$$

$$T_m = 1680 \text{ K};$$

$$Q_{cp} = \begin{cases} 0.65 \cdot 270 \text{ KJ/mol}, & \text{if } T < 840 \text{ K} \\ 270 \text{ KJ/mol}, & \text{if } T > 840 \text{ K} \end{cases}$$

$$n_c = 1.13$$